Figure-Eight Tetrathiaoctaphyrin and Dihydrotetrathiaoctaphyrin

Natasza Sprutta and Lechosław Latos-Grażyński*[a]

Abstract: The acid-catalyzed condensation of pyrrole and 2,5-bis(*p*-tolylhydroxymethyl)thiophene yields two novel giant heteroporphyrins: 5,10,15,20,25,30,35,40-octa(*p*-tolyl)-41,43,45,47-tetrathia-[36]octaphyrin(1.1.1.1.1.1.1.1) (S_4OP) and 5,10,15,20,25,30,35,40-octa(*p*-tolyl)-dihydro-41,43,45,47-tetrathia[38]octaphyrin(1.1.1.1.1.1.1.1) (S_4OPH_2). These tetrathiaoctaphyrins are interconvertible through dihydrogenation or dehydrogenation processes. Both compounds possess helical figure-eight geometry with two thiophene rings for S_4OP or two pyrrole rings for S_4OPH_2 in the ribbon-crossing center as shown by NOESY experiments. The synthesis of the figure-eight tetrathiaoctaphyrin implies a prearrangement process to form helical *M* or *P* dithiatetrapyrromethanes. The *P*–*P* or *M*–*M* condensation leads to the figure-eight molecule in competition with an intramolecular ring closure. Two dithiaporphyrin-like pockets of S_4OP or S_4OPH_2 behave as independent proton acceptors. The stepwise process yields symmetric or asymmetric cationic species that depends on whether an even or odd number of NH protons are added. Dihydrotetrathiaoctaphyrin contains 38 π electrons in its conjugation pathway, which corresponds to the formal $[4n+2]$ Hückel type π-electron formulation that is consistent with a modest diatropic ring current effect in their ^{1}H NMR spectra. The formal $4n$ type π-electron formulation for tetrathiaoctaphyrin accounts for the residual paratropic shifts. A figure-eight conveyor-belt-like movement of the whole macrocyclic ring without a racemization step is proposed to account for the dynamic properties of S_4OP. The molecule shuttles between two degenerate configurations.

A S_4OP–S_4OPH_2 couple may be considered as a molecular element which, while preserving the overall figure-eight geometry, "chooses" pyrrole or thiophene rings as spacers as a function of the macrocyclic oxidation state.

Keywords: macrocycles · NMR spectroscopy · porphyrinoids · sulfur heterocycles

Introduction

A renewal of the Rothemund type synthesis has been used to produce "giant" porphyrins, which contain more than six pyrrole moieties.[1, 2] Their synthesis has been based on the general acid condensation which involves aryl aldehydes and bipyrrolic units with blocked β-pyrrolic positions.[1] Originally, Sessler and co-workers demonstrated that the acid-catalyzed condensation of tetraalkylbipyrrole and aryl aldehyde yielded [24]hexaphyrin(1.0.1.0.1.0) (rosarin).[3] Recently, Setsune et al. reported that in a related condensation with *ortho*-substituted benzaldehydes, [32]octaphyrin(1.0.1.0.1.0.1.0), [48]decaphyrin(1.0.1.0.1.0.1.0.1.0), and [64]hexadecaphyrin-(1.0.1.0.1.0.1.0.1.0.1.0.1.0.1.0) were formed.[1a] The bipyrrolic fragments are bridged by methine fragments, which are substituted with aryl rings. Alternatively, the condensation of bis(azafulvene) and bipyrrole led to the synthesis of [80]icosaphyrin(1.0.1.0.1.0.1.0.1.0.1.0.1.0.1.0.1.0.1.0.1.0) and [96]tetracosphyrin(1.0.1.0.1.0.1.0.1.0.1.0.1.0.1.0.1.0.1.0.1.0.1.0.1.0).[1b] The fact that these expanded porphyrins are synthesized by a relatively simple methodology from commonly accessible substrates creates an opportunity for further extensive studies on the coordination chemistry and anion-binding properties. The *meso*-arylated expanded porphyrins are related to expanded porphyrins in which pyrrolic fragments are linked by direct C_α–C_α bonds or by unsubstituted *meso*-methine $(CH)_n$ units ($n=1$, 2). This class includes the following macrocycles: [28]heptaphyrin(1.0.0.1.0.0.0),[4] [32]octaphyrin(1.0.1.0.1.0.1.0),[5] [32]octaphyrin(1.0.0.0.1.0.0.0),[4] [34]octaphyrin(1.1.1.0.1.1.1.0),[6] [36]octaphyrin(2.1.0.1.2.1.0.1),[6, 7] and [40]decaphyrin(0.0.1.0.1.0.0.1.0.1) (turcasarin).[8] A heteroanalogue of turcasarin – dioxaturcasarin has also been synthesized.[9] In addition, Cava and co-workers have synthesized the decaheterocyclic nonaromatic macrocycle hexathia[44]decaphyrin(2.0.0.0.0.2.0.0.0.0) and its *N*,*N*′-linked derivative.[10] *meso*-Aryl heteroheptaphyrins (1.1.0.0.1.1.0) and (1.0.1.0.1.1.0.0), which contain seven heterocyclic rings, are aromatic.[11] Fully conjugated macrocyclic oligothiophenes, which contain up to 18 thiophene units, have recently been reported.[12]

Since the first synthesis reported by Rothemund, 5,10,15,20-tetraphenylporphyrin[13] and its aryl and alkyl analogues

[a] Professor L. Latos-Grażyński, N. Sprutta
Department of Chemistry
University of Wrocław
14 F. Joliot -Curie St.
Wrocław 50383 (Poland)
Fax: (+71) 3-282-348
E-mail: LLG@wchuwr.chem.uni.wroc.pl

  0947-6539/01/0723-5099 $ 17.50+.50/0

have been synthesized by a variety of procedures that are based on the same principle, which involves the one- and two-step condensation of pyrrole and an aldehyde of choice.[14] A similar approach was used by Ulman and Manassen in their seminal work on the synthesis of 5,10,15,20-tetraphenyl-21,23-diheteroporphyrins.[15] Their strategy was based upon an analogous mechanism of the ordinary acid-catalyzed reaction between arylaldehyde and pyrrole, in which the 2,5-bis(arylhydroxymethyl)pyrrole was suggested as an intermediate.[15a] Consequently the reaction between 2,5-bis(arylhydroxymethyl)heterocyclopentadienes and pyrroles in acidic media produced a variety of 21,23-diheteroporphyrins in which the NH groups were replaced with oxygen, sulfur, selenium or tellurium atoms.[15, 16] Once arylaldehyde was included in a condensation, 5,10,15,20-tetraaryl-21-heteroporphyrins were also produced.[16–18] Instead of pyrrole and benzaldehyde a variety of *meso*-substituted dipyrromethanes were used as a building block in the condensation with 2,5-bis(phenylhydroxymethyl)furan or 2,5-bis(phenylhydroxymethyl)thiophene to produce monoheteroporphyrins.[19a] A [3 + 1] condensation involving 5,10-diphenyl-16-thiatripyrrane and 2,5-bis(phenylhydroxymethyl)furan offered an alternative efficient synthetic route to *meso*-aryl-substituted heteroporphyrins.[19b]

The accessibility of 5,10,15,20-tetraaryl-2-aza-21-carbaporphyrin in the reaction of arylaldehyde with pyrrole gave rise to the revision of the view that tetraarylporphyrin is the sole macrocyclic product of the Rothemund-type synthesis.[17, 20–23] Subsequently, apart from tetraarylporphyrin and inverted tetraarylporphyrin,[20] three other aromatic macrocycles have been identified among the products of the pyrrole – arylaldehyde condensation: tetraarylsapphyrin,[21] trisarylcorrole,[22] *meso*-hexa(pentafluorophenyl)hexaphyrin(1.1.1.1.1.1)[23] and—as observed recently—dodecaphyrin.[24]

We have previously established that the routine procedures, that is the condensation of pyrrole, arylaldehyde, and 2,5-bis(arylhydroxymethyl)furan or 2,5-bis(arylhydroxymethyl)-thiophene, produces 5,10,15,20-tetraaryl-26,28-dioxasapphyrin, 5,10,15,20-tetraaryl-26,28-dithiasapphyrin as well as 5,10,15,20-tetraaryl-21-oxaporphyrin and 5,10,15,20-tetraaryl-21-thiaporphyrin.[25] Remarkably, the acid-catalyzed condensation of 16-oxatripyrrane, 16-thiatripyrrane, or 16-selenatripyrrane gave 18-π, 22-π, and 26-π macrocycles (*meso*-aryl diheteroporphyrins, diheterosapphyrins, and diheterorubyrins).[26] A condensation of 5-(*p*-tolyl)dipyrromethane and furylpyrromethanediol gave 5,10,15-trisaryl-21-oxacorrole in addition to 5,10,15,20-tetraaryl-21-oxaporphyrin.[27]

The discovery of "giant" porphyrins resulted in the anticipation that a combination of any other building blocks, which are typically used in acid condensation synthesis of porphyrin or heteroporphyrin, is likely to yield "giant" heteroporphyrins. Consequently, condensation of bis(arylhydroxymethyl)heterocyclopentadienes and pyrrole may provide a path to expanded *meso*-aryl heteroporphyrins of the general formula presented in Scheme 1.

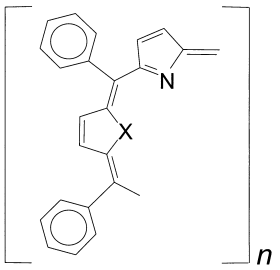

Scheme 1. General formula of the expanded *meso*-aryl heteroporphyrins.

We report herein on a route to expanded thiaporphyrins (X = S) which provides the first *meso*-octa(*p*-tolyl)tetrathia[36]octaphyrin(1.1.1.1.1.1.1.1) and its dihydrogenation product *meso*-octa(*p*-tolyl)dihydrotetrathia[38]octaphyrin-(1.1.1.1.1.1.1.1). Thus, we describe the properties of two novel helical figure-eight macrocycles.

Abstract in Polish: *W wyniku katalizowanej kwasem kondensacji pomiądzy pirolem a 2,5-bis(p-toluilohydroksymetylo)tiofenem powstaję dwie nowe "gigantyczne" porfiryny - 5,10,15,20,25,30,35,40-okta(p-toluilo)-41,43,45,47-tetratia[36]-oktafiryna(1.1.1.1.1.1.1.1), S_4OP, oraz 5,10,15,20,25,30,35,40-okta(p-toluilo)-dihydro-41,43,45,47-tetratia[38]oktafiryna(1.1.1.1.1.1.1.1), S_4OPH_2. Wykazano, że mogą one przechodzić w siebie wzajemnie na drodze hydrogenacji - dehydrogenacji. Oba zwiazki przyjmuję konformacją ósemki co udowodniono na podstawie eksperymentów ^1H NMR COSY i NOESY. Dwa pierścienie tiofenowe dla S_4OP i dwa pirolowe dla S_4OPH_2 znajdują się na przecięciu "ósemki". Każdy z ditiaporfirynopodobnych fragmentów S_4OP lub S_4OPH_2 zachowuje się jako niezależny akceptor protonów. Stopniowa protonacja prowadzi do symetrycznej (w przypadku parzystej liczby dodanych protonów) lub asymetrycznej (w przypadku nieparzystej liczby dodanych protonów) formy kationowej. Ścieżka aromatyczności dihydrotetratiaoktafiryny (38 elektronów π) wskazuje, zgodnie z regułą Hückla (4n + 2), na układ z diatropowym efektem pradu pierścieniowego, co przejawia się w widmach ^1H NMR odpowiednim przesunięciem linii rezonansowych. Analogicznie 4n elektronów π (n = 9) dla tetratiaoktafiryny tłumaczy obecność efektu paratropowego. Zaproponowano nowy mechanizm wyjaśniający tłumaczący dynamiczne właściwości S_4OP. Wymaga on ruchu całego makrocykla analogicznego do ruchu taśmy przenośnikowej. Ruch taki zachodzi z zachowaniem skrętności ósemki. Układ $S_4OP – S_4OPH_2$ można uznać za molekularny przełącznik, którego działanie jest oparte o chemię utleniania i redukcji. Zależnie od stopnia utlenienia makrocykla umieszcza on pirol lub tiofen w miejscu skrzyżowania "ósemki".*

Results and Discussion

Synthesis and characterization:

5,10,15,20,25,30,35,40-Octa(*p*-tolyl)-41,43,45,47-tetrathia-[36]octaphyrin(1.1.1.1.1.1.1.1) (S_4OP) has been obtained by a procedure which is analogous to that applied to obtain 5,10,15,20-tetraphenyl-21,23-dithiaporphyrin (S_2TPPH) and 5,10,15,20-tetraphenyl-26,28-dithiasapphyrin (S_2TPSH).[15a, 15e, 18a, 25] The mechanistic considerations, which relate to the synthesis of 5,10,15,20-tetraphenyl-21,23-dithiaporphyrin have been taken into account in the resultant schematic synthetic route presented in Scheme 2.

The synthesis involves the one-pot reaction of 2,5-bis(*p*-tolylhydroxymethyl)thiophene with pyrrole in dichloromethane (1:1 molar ratio), which is catalyzed by methanesulfonic

0947-6539/01/0723-5100 $ 17.50+.50/0 *Chem. Eur. J.* **2001**, *7*, No. 23

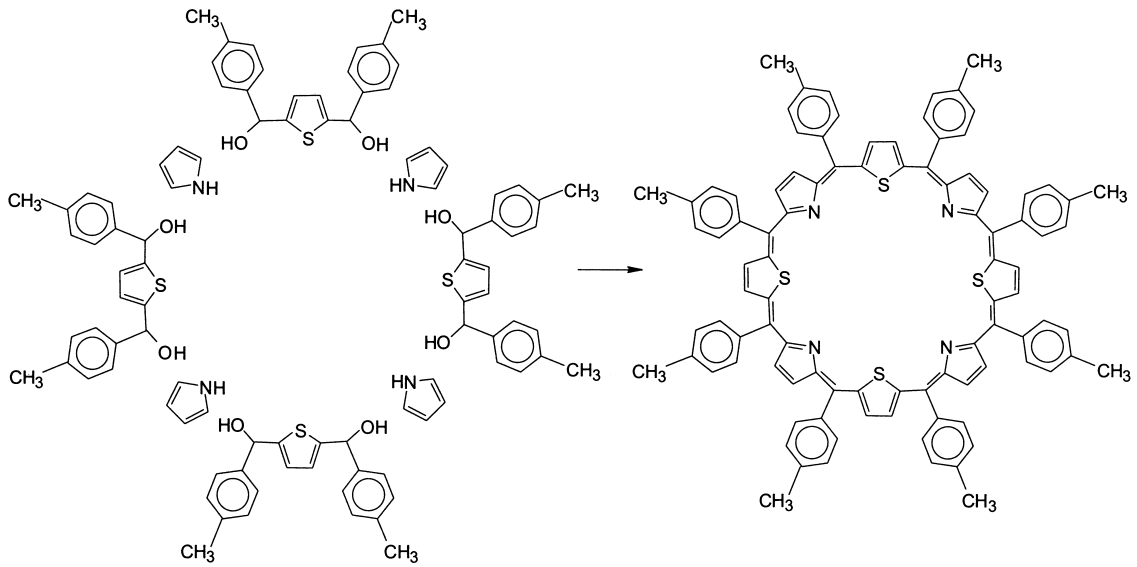

Scheme 2. Synthetic route to 5,10,15,20,25,30,35,40-octa(*p*-tolyl)-41,43,45,47-tetrathiooctaphyrin.

acid and which is followed by oxidation by *p*-chloranil. The choice of the *p*-tolyl derivative is of importance in the further spectroscopic and structural analysis.

The condensation process produces, in addition to 5,10,15,20-tetra(*p*-tolyl)-21,23-dithiaporphyrin, other aromatic macrocyclic derivatives which include the previously characterized 5,10,15,20-tetra(*p*-tolyl)-26,28-dithiasapphyrin (26,28-S_2TTSH)[25] and the novel 5,10,15,20-tetra(*p*-tolyl)-25,27-dithiasapphyrin (25,27-S_2TTSH). 22,24-Dithiaporphyrin with an inverted pyrrole ring, 5,10,15,20-tetra(*p*-tolyl)-2-aza-21-carba-22,24-dithiaporphyrin (S_2CTTP), is also identified.[28]

We isolated the following by careful examination of all fractions that were obtained by chromatography on basic alumina: 5,10,15,20,25,30,35,40-octa(*p*-tolyl)-41,43,45,47-tetrathia[36]octaphyrin(1.1.1.1.1.1.1.1) (S_4OP) in 2% yield. In this series of experiments the formation of S_4OP is usually accompanied by a second derivative which contains two more hydrogen atoms: 5,10,15,20,25,30,35,40-octa(*p*-tolyl)-dihydro-41,43,45,47-tetrathia[38]octaphyrin(1.1.1.1.1.1.1.1), that is dihydrotetrathiaoctaphyrin (S_4OPH_2) (Scheme 3).

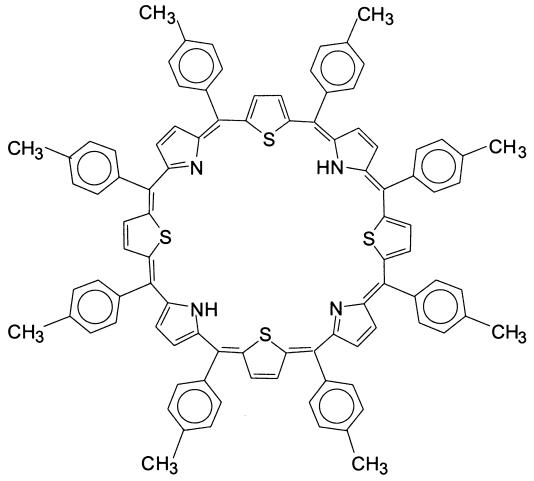

Scheme 3. Dihydrotetrathiaoctaphyrin (S_4OPH_2).

Once identified and thoroughly characterized, both tetrathiaoctaphyrins are detected in other condensations which included 2,5-bis(arylhydroxymethyl)thiophene and pyrrole. For instance S_4OP and S_4OPH_2 have been obtained in Lindsey conditions using $BF_3 \cdot Et_2O$ as a catalyst. S_4OP and S_4OPH_2 demonstrate strikingly different affinities toward basic alumina in the course of column chromatography. The distinct marine-green fraction, which contains S_4OP, elutes with dichloromethane from the basic alumina column just after its lower homologue, S_2TTP. The green fraction, which contains S_4OPH_2, elutes with the polar mixture chloroform/methanol (90/10 *v*/*v*) initially with some residual tarry products.

Both tetrathiaoctaphyrins, S_4OP and S_4OPH_2, are interconvertible. S_4OP undergoes dihydrogenation by using sodium borohydride in THF to form S_4OPH_2 in a quantitative manner. Well-defined isosbestic points are detected for the process which was followed by UV spectroscopy. Dihydrogenation has been used to produce S_4OPH_2 on a synthetic scale. The reaction of S_4OP with sodium hyposulfite in a biphasic dichloromethane/water system also produces S_4OPH_2. Notably, oxidation of S_4OPH_2 by *p*-chloranil or 2,3-dichloro-5,6-dicyano-1,4-benzoquinone (DDQ) yields S_4OP.

Mass spectrometry of S_4OP suggests the empirical formula $C_{96}H_{72}N_4S_4$ which is consistent with presence of four [C(C_6H_4-(*p*-CH_3))]-(C_4H_2S)-[C(C_6H_4(*p*-CH_3))]-(C_4H_2N) fragments in the molecule (Scheme 2). The empirical formula of S_4OPH_2, $C_{96}H_{74}N_4S_4$, also accounts for the presence of four [C(C_6H_4(*p*-CH_3))]-(C_4H_2S)-[C(C_6H_4(*p*-CH_3))]-(C_4H_2N) units with addition of two NH hydrogen atoms (Scheme 3).

Spectroscopic characterization of S_4OP and S_4OPH_2: The electronic spectrum of S_4OP shows two major bands of the comparable intensities at 427 and 631 nm (Figure 1). In contrast with porphyrins and aromatic expanded porphyrins, the intense Soret-like band is absent. The electronic spectrum of S_4OPH_2 resembles that of S_4OP although the longer wavelength band is bathochromically shifted to 739 nm positions (Figure 1). The S_4OP and S_4OPH_2 patterns of

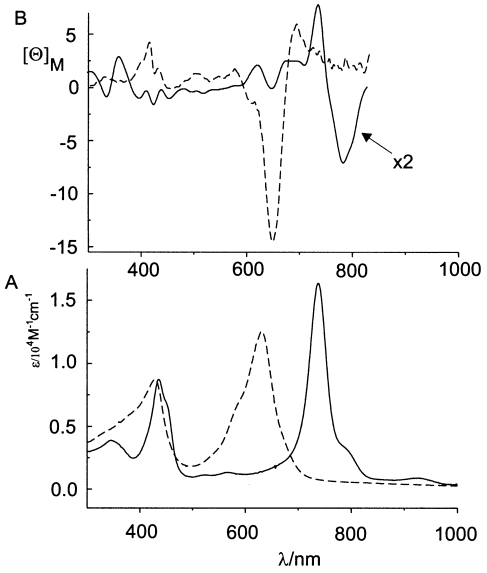

Figure 1. Trace A: The electronic spectra of S_4OPH_2 (solid line), S_4OP (dashed line) in dichloromethane. Trace B: The MCD spectra at 293 K, 0.1437 T of S_4OPH_2 (solid line) and S_4OP (dashed line) in dichloromethane.

electronic spectra are similar to those of [34]octaphyrin(1.1.1.0.1.1.1.0).[29] The magnetic circular dichroism (MCD) spectra of S_4OP and S_4OPH_2 has features at positions which correspond to positions of the absorption bands in the electronic spectrum (Figure 1).

Representative ^{1}H NMR spectra of S_4OP are shown in Figure 2. The neutral form of S_4OP produces well-resolved spectra but only under certain optimized conditions. The visibility of diagnostic features depends strongly on a choice of solvent and temperature. Severe broadening of all resonances, particularly in the $\delta = 10-6$ region, is observed at 298 K in $[D_2]$dichloromethane, [D]chloroform or $[D_8]$toluene (Figure 2, Trace C).

The assignments of the S_4OP resonances, which are given above selected groups of peaks (Figure 2 Trace A) and shown in Table 1, are made on the basis of relative intensities and of detailed two-dimensional ^{1}H NMR studies (COSY, NOESY) carried out at 213 K in $[D_2]$dichloromethane. The site-specific deuteration of the pyrrole moieties ($[D_8]S_4OP$) and exchange of labile NH protons by deuterons to form ND in the presence of D_2O (in the case of the $S_4OPH_n^{n+}$ cationic species) is used as an independent route of assignments. The ^{1}H NMR spectrum of S_4OP (213 K) exhibits four AB patterns. Two of them ($\delta =$ 6.17, 6.49; 6.47, 6.60) are easily assigned to the β-H pyrrole protons as they are extremely diminished in the corresponding spectrum of $[D_8]S_4OP$. By default, the two other AB patterns are assigned to the thiophene rings. Four different sets of *meso-p*-tolyl ring resonances are observed. Each demonstrates two *ortho* and two *meta* resonances readily correlated through COSY and NOESY techniques with particular methyl resonances. The differentiation of *ortho* and *meta* resonances suggests that the *p*-tolyl rotation with respect to the C_{meso}–C_{phenyl} bond is slow below 213 K and that the tetrathiaoctaphyrin macrocycle is not planar. Importantly, the multiplicity of all resonances is identical even at 193 K in

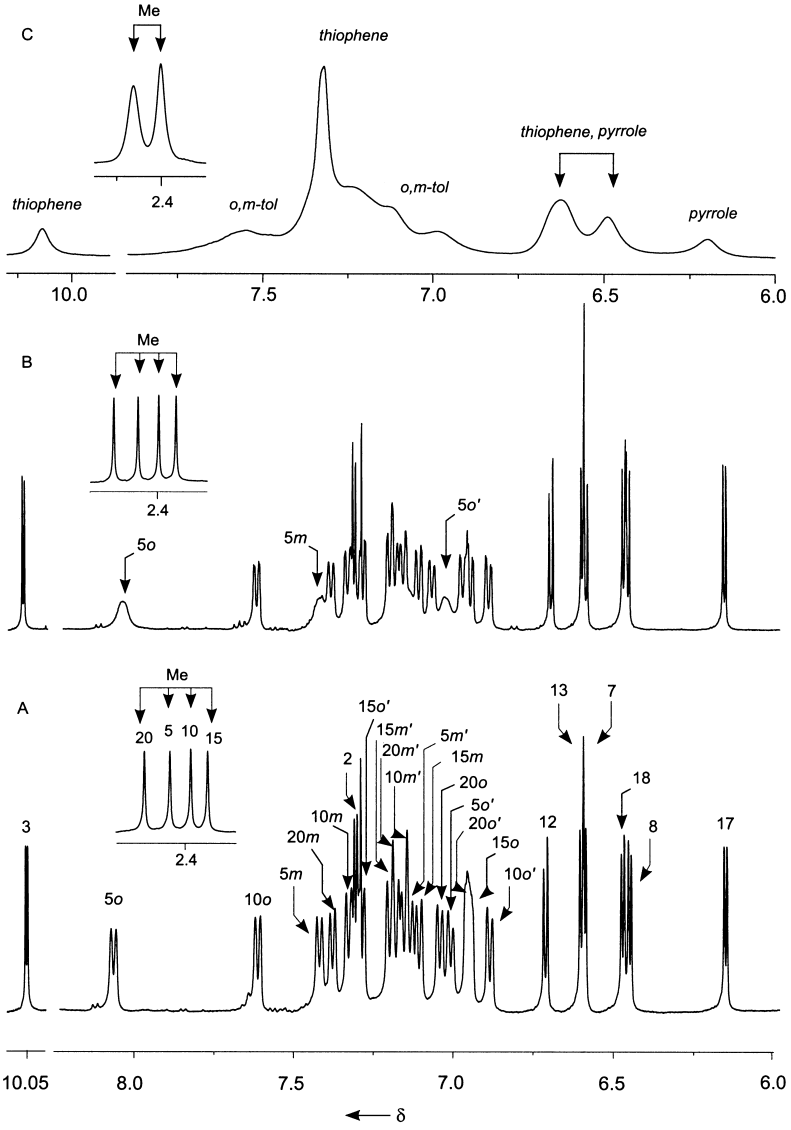

Figure 2. ^{1}H NMR spectra (selected downfield and upfield regions only) of S_4OP at 213 (A), 243 (B), and 298 K (C) in $[D_2]$dichloromethane. Inset: *p*-methyl resonances. Peak labels follow systematic position numbering of the tetrathiaoctaphyrin ring or denote proton groups: *o*, *m*, denotes *ortho*, *meta*, positions of *meso p*-tolyl rings, respectively.

0947-6539/01/0723-5102 $ 17.50+.50/0 *Chem. Eur. J.* **2001**, *7*, No. 23

Table 1. ^{1}H NMR data of S_4OP and S_4OPH_2.

Position	$\delta(^1H)$		$\Delta\delta(^1H)$[c]
	S_4OP[a]	S_4OPH_2[b]	
2-H	7.32	7.51	– 0.19
3-H	10.05	6.97	2.42
7-H	6.60	4.18	2.10
8-H	6.47	4.37	– 0.08
12-H	6.73	6.81	– 0.92
13-H	6.62	7.54	– 0.83
17-H	6.17	7.00	-0.51
18-H	6.49	7.00	3.08
5*o*	8.08	5.46	2.6
5*o*′	7.02	7.52	– 0.50
5*m*	7.44	6.47	0.97
5*m*′	7.15	7.04	0.11
10*o*	7.63	4.46	3.17
10*o*′	6.90	8.25	– 1.3
10*m*	7.35	6.43	0.92
10*m*′	7.17	5.27	1.90
15*o*	6.96	7.94	– 0.98
15*o*′	7.30	6.94	0.36
15*m*	7.12	7.48	– 0.3
15*m*′	7.22	7.24	– 0.02
20*o*	7.06	7.50	– 0.44
20*o*′	6.98	7.28	– 0.30
20*m*	7.40	7.43	– 0.03
20*m*′	7.20	7.30	– 0.10
p-methyl			
5	2.44	2.30	0.14
10	2.38	1.36	1.02
15	2.33	2.47	– 0.14
20	2.52	2.48	0.04
NH	-	5.36	-

[a] $\delta(^1H)$ for S_4OP at 213 K. [b] $\delta(^1H)$ for S_4OPH_2 at 253 K. [c] $\Delta\delta(^1H) = \delta(S_4OP) - \delta(S_4OPH_2)$.

[D_2]dichloromethane. In general the ^{1}H NMR spectroscopic pattern is consistent either with C_i or C_2 symmetry of tetrathiaoctaphyrin. Eight AB patterns and eight *p*-methyl resonances are expected for a molecule without any element of symmetry. The C_s symmetry of tetrathiaoctaphyrin can be excluded as it implies the magnetic equivalence of pyrrole (thiophene) protons, which are located on the same ring. The existence of A_2 pattern(s) in the NMR spectrum of S_4OP is required for such geometry.

Crystal and solution structures of octaphyrins demonstrate a helical figure-eight arrangement of their skeletons.[5, 6, 7] A chiral figure-eight conformation of expanded porphyrins was originally discovered in turcasarin.[8] These molecules exist in a chiral figure-eight conformation in the crystal and the sense of rotation of the resulting helix is designated with the description *P* for the right-handed and *M* for the left-handed orientation.[30] Molecules with a figure-eight conformation are known in other fields. Such geometry has been determined for propellicenes[31] and [28]paracyclophaneoctaene.[32] This motif has been also observed among cyclic peptides[33] and coordination compounds.[34]

The structural formula of S_4OP shown in Scheme 2 demonstrates that the planar circular structures which facilitate a π-electron count. To account for the ^{1}H NMR spectra that are characteristic of S_4OP nonplanar structural scaffolds, a C_2 figure-eight-shaped double helical fold is considered (Scheme 4). In the construction of models, it is accepted that five-member rings of expanded porphyrins can adopt the regular and 180° inverted or "flipped" positions.

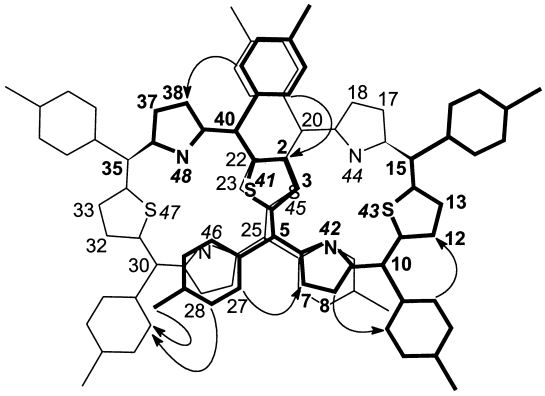

Scheme 4. Structurally important dipolar relays of figure-eight geometry of S_4OP(arrows).

Molecular mechanics calculations have been used to visualize the suggested structures of tetrathiaoctaphyrin and to assess the degree of the macrocycle distortion that is necessary to form this species (Figure 3). The figure-eight

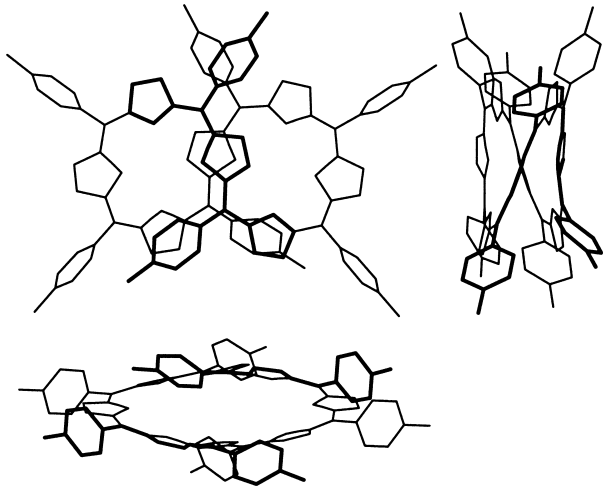

Figure 3. Structure of S_4OP from molecular mechanics calculations.

twist defines two dithiaporphyrin-like macrocycles. The ribbon crossing of S_4OP consists of two thiophene-S(41) and thiophene-S(45) moieties that belong to upper and bottom part of the "macrocyclic ribbon" as the molecule possesses C_2 symmetry. The corresponding skeleton (Scheme 4) highlights that S(41) and S(45) thiophene rings are oriented in the opposite direction. Consequently 3-H hydrogen and 23-H hydrogen atoms are directed toward the centers of dithiaporphyrin-like pockets. The 3-H and 23-H positions are quite unique for the whole molecule. They are diagnostic of the "zigzag" fragment of the skeleton. The assignment of these two resonances provided the starting point for the analysis of the COSY and NOESY experiments. The 2D NMR studies

were preceded by initial assignments from the selective deuteration at β-pyrrole positions (Table 1). The resulting fundamental relays of observed and assigned COSY and NOE connectivities are presented at Scheme 4. Here we only present the most fundamental steps of the spectroscopic discussion, which is based on the structural constraint of the figure-eight geometry. The spatial proximity of the 2-H – 40-*p*-tolyl and 3-H – 5-*p*-tolyl implies strong NOE cross-peaks exclusively between 2-H(thiophene) and *ortho*-H(40-*p*-tolyl). The figure-eight geometry requires a *trans* arrangement of 5-*p*-tolyl and 3-CH moieties with respect to the C(4)–C(5) bond contrary to the cis arrangement in the regular heteroporphyrin. Thus, the 3-H(thiophene) and *ortho*-H(5-*p*-tolyl) are the only pair in the whole structure where the β-H and the adjacent *ortho*-H(*p*-tolyl) distance is too large to allow efficient dipolar coupling. Characteristic sets of contacts are expected at other fragments of S_4OP. In comparison to the 2-H – 3-H pair, the 12-H and 13-H thiophene protons reveal connectivity to *ortho*-H(*p*-tolyl) protons (12-H – *ortho*-H(10-*p*-tolyl) and 13-H – *ortho*-H(15-*p*-tolyl), respectively). Additionally, the *ortho* protons of 10,15,20-*p*-tolyl rings are adjacent to two different β-H protons: the first originates from the pyrrole ring and the second from the thiophene ring. Due to their spatial proximity, the unique cross peak between $\delta = 7.32$ (pyrrole) and 7.40 (*ortho*) allows their assignment as 2-H and *ortho*-H(40-*p*-tolyl), respectively. The 3-H resonance is located at $\delta = 10.05$ as confirmed by a 2-H – 3-H COSY cross-peak. As predicted, there is no NOE correlation to this particular resonance, which originates from the 5-*p*-tolyl fragment. The 5-*p*-tolyl ring is identified by default, as this is a unique *p*-tolyl ring, with a single strong β-H – *ortho*-H cross-peak (7-H(pyrrole) – *ortho*-H(5-*p*-tolyl)). The specific helical structure of S_4OP imposes the close proximity of *p*-methyl(5-*p*-tolyl) and *ortho*-H(30-*p*-tolyl) protons ($\approx$ 2.98 Å from the *MM*+ model) which contrasts with the very large *p*-methyl(5-*p*-tolyl) and *ortho*-H(10-*p*-tolyl) distance (at least 10 Å). In addition, *meta*-H(5-*p*-tolyl) and *ortho*-H(30-*p*-tolyl) are adjacent ($\approx$ 2.2 – 3.1 Å from the *MM*+ model, depending on the orientation of the ring). Similarly 3-H and *ortho*-H of 25-*p*-tolyl are closely situated. As a consequence, a NOE cross-peak between the *p*-methyl (2.44 ppm) and *ortho*-H (7.63 ppm) resonances, which reflects the methyl(5-*p*-tolyl) – *ortho*-H(30-*p*-tolyl) contact, is detected in the NOE map. Analogously, the *meta*-H(5-*p*-tolyl) – *ortho*-H(30-*p*-tolyl) and 3-H – *ortho*-H(25-*p*-tolyl) dipolar interactions can also be correlated. It is important to notice these sets of correlation serve as definitive structural markers of the figure-eight helical structure.

Spectroscopic characterization of S_4OPH_2: The representative ^{1}H NMR spectral patterns of S_4OPH_2 are shown in Figure 4. Severe broadening of all *p*-tolyl resonances is observed at 298 K in [D_2]dichloromethane or [D_8]toluene but well-resolved spectra are collected at 253 K.

The assignments of the S_4OPH_2 resonances, which are given above selected groups of peaks (Figure 4, Trace A) and listed in Table 1, were carried out in a similar manner to those for S_4OP, including the selective deuteration of β-pyrrole and NH positions to give [D_8]S_4OPH_2 and S_4OPD_2, respectively. Indeed the ^{1}H NMR spectroscopic pattern of S_4OPH_2 reflects the multiplicity and connectivity expected for the C_2 figure-eight geometry. There is, however, one crucial structural difference between S_4OP and S_4OPH_2. Specifically, dihydrogenation of S_4OP to S_4OPH_2 is accompanied by a replacement of a thiophene fragment by a pyrrole fragment at the ribbon crossing location. All structurally important dipolar and scalar relays of figure-eight geometry, which are observed for S_4OP, are observed in the case of S_4OPH_2 as shown by arrows in Scheme 5. However, the most important spatial contacts for the structure determination are provided by the following

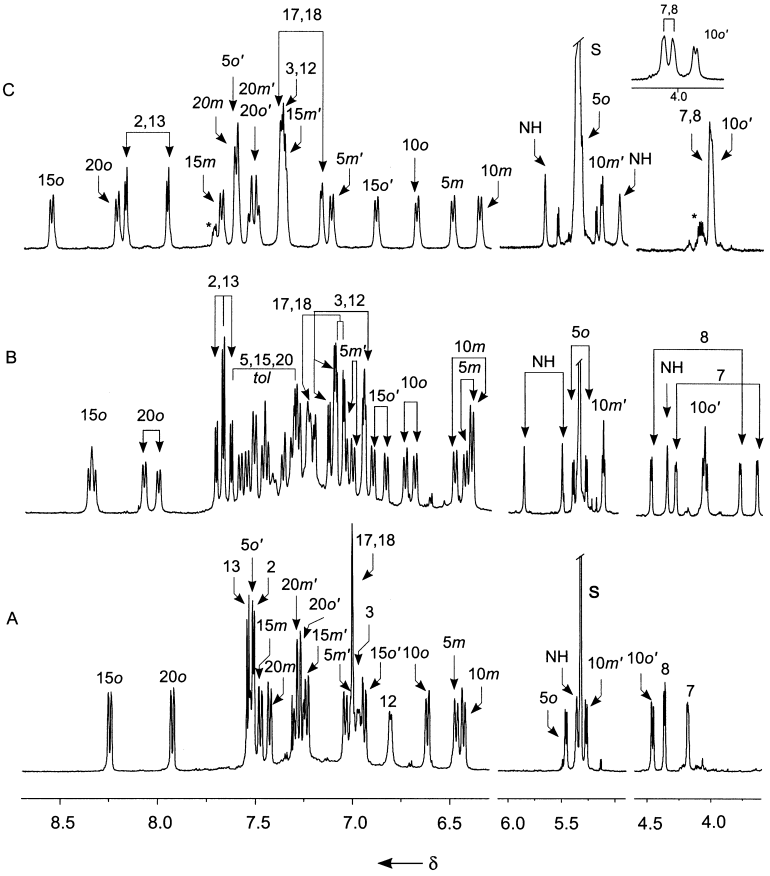

Figure 4. ^{1}H NMR spectra (selected downfield and upfield regions only): A) S_4OPH_2 (253 K), B) $S_4OPH_3^+$ (218 K), C) $S_4OPH_4^{2+}$ (213 K) obtained by titration with trifluoroacetic acid (TFA) in [D_2]dichloromethane. Inset: from Trace C presents the fragment of the $S_4OPH_4^{2+}$ spectrum as measured at 273 K. Labeling as in Figure 2.

0947-6539/01/0723-5104 $ 17.50+.50/0 *Chem. Eur. J.* **2001**, *7*, No. 23

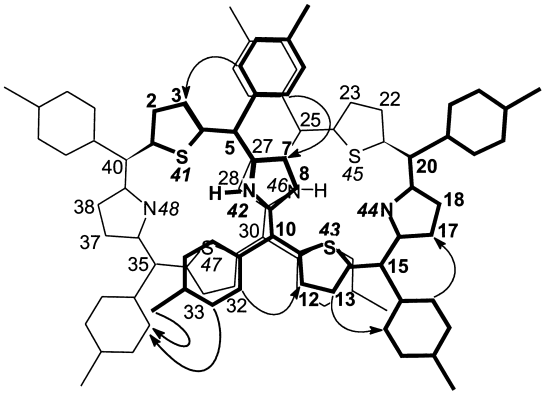

Scheme 5. Structurally important dipolar relays of figure-eight geometry of S_4OPH_2 (arrows).

pairs: methyl(10-*p*-tolyl)–*ortho*-H(35-*p*-tolyl), *meta*-H(5-*p*-tolyl)–*ortho*-H(35-*p*-tolyl), and 7-H–*ortho*-H(5-*p*-tolyl).

In spite of the scaffolding similarities, the spectroscopic pattern of S_4OPH_2 is markedly different from that of S_4OP as evident from the comparison of Figure 2 and Figure 4. The downfield bias of the selected resonances seen for S_4OP has been replaced by an upfield trend in S_4OPH_2 (Table 1).

Protonation and tautomeric equilibria: A ^{1}H NMR titration of S_4OPH_2 {[48-N,42-NH][44-N,46-NH]} with trifluroacetic acid (TFA) in [D_2]dichloromethane results in the gradual formation of a monocationic form, followed by a dication (Figure 4 and Figure 5).

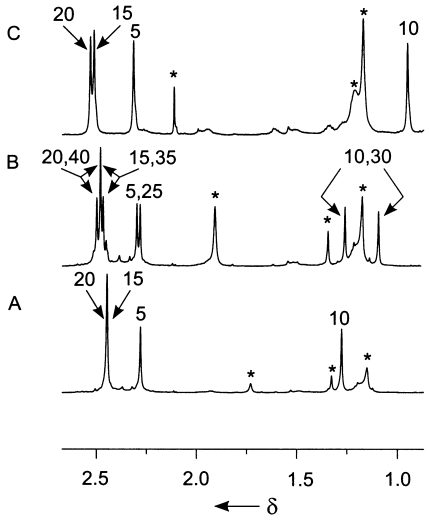

Figure 5. The *p*-methyl regions of ^{1}H NMR spectra for A) S_4OPH_2 (253 K), B) $S_4OPH_3^+$ (218 K), C) $S_4OPH_4^{2+}$ (213 K) obtained by titration with TFA in [D_2]dichloromethane. * denotes solvent impurities.

The protonation mechanism reflects the unusual structure of the molecule. The addition of the first proton removes the equivalency of the two dithiaporphyrin-like pockets. Consequently, a double number of resonances is detected in the spectrum of $S_4OPH_3^+$ with respect to that of S_4OPH_2. An appearance of the N(44)H resonance and differentiation of N(42)H and N(46)H resonances accompany this process. One subset corresponds to the protonated part and the second preserves the features of the original molecule (Figure 4, Trace B, and Figure 5, trace B). The pattern of the *p*-methyl resonances can be treated as a structurally diagnostic "fingerprint" of the $S_4OPH_{2+n}^{n+}$ cationic forms (Figure 5). Thus, eight *p*-methyl resonances have been readily identified for $S_4OPH_3^+$ (Figure 5, Trace B). The symmetrically protonated form, $S_4OPH_4^{2+}$, is shown by a set of four *p*-methyl resonances (Figure 5, Trace C). The odd number of NH protons lowers the symmetry of the cation, as shown in ^{1}H NMR spectra. This would not be observed in the fast exchange of NH protons between two pockets.

Parallel studies carried out for S_4OP revealed similar behaviour (Figure 6). Addition of the first proton produces the asymmetric S_4OPH^+, which doubles the resonance peaks.

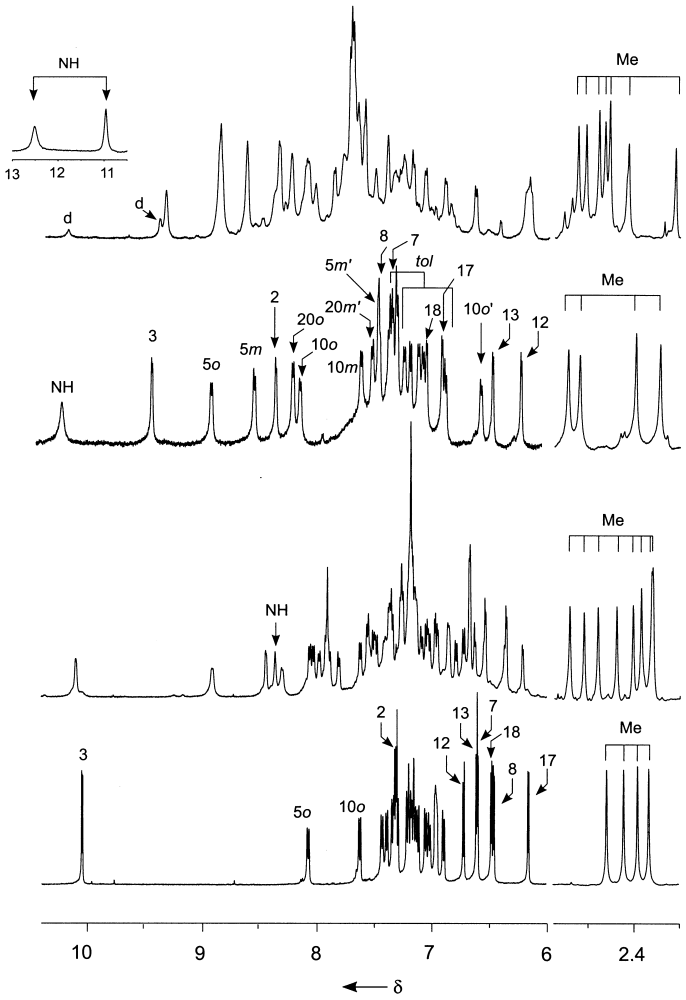

Figure 6. ^{1}H NMR spectra of A) S_4OP (213 K), B) S_4OPH^+ (203 K), C) $S_4OPH_2^{2+}$ (196 K), D) $S_4OPH_3^{3+}$ (203 K, the eighth methyl resonance at $\delta = 0.53$, d – a dicationic species) obtained by titration of S_4OP with TFA in [D_2]dichloromethane. Inset from Trace D contains two NH resonances of $S_4OPH_3^{3+}$ (the third NH resonance has not been identified). Labeling as in Figure 2.

This implies the formation of a single tautomer, presumably {[42-N,44-NH][46-N,48-N]} which avoids the CH–NH *cis* interaction which is expected for {[42-NH,44-N][46-N,48-N]}. Alternatively this behavior can be explained with the assumption that S_4OP, like many other porphyrins, is subject

to NH tautomerism which involves two forms: {[42-NH, 44-N]-[46-N, 48-N]} and {[42-N, 44-NH][46-N, 48-N]}. The fast tautomerization should be limited to the single dithiaporphyrin-like pocket without the possibility of fast interpocket proton exchange. An attempt to lower the possible exchange rate was made by measuring the spectrum at 193 K, but without any effect that could be related to the formation of two alternative monocationic forms. The next titration step produces a symmetric dication followed by an asymmetric trication $S_4OPH_3^{3+}$. Consistent with symmetry of the prevailing species in solution, alternately four, eight, four, and eight methyl resonances are detected for S_4OP, S_4OPH^+, $S_4OPH_2^{2+}$, and $S_4OPH_3^{3+}$ in the course of titration (Figure 6).

Aromaticity and antiaromaticity of figure-eight tetrathiaoctaphyrins: The most obvious differences between S_4OPH_2 and S_4OP ^{1}H NMR spectra are revealed at the figure-eight crossing fragments: S_4OP, [C(40)(C_6H_4-CH_3)]-[C_4H_2S(41)]-[C(5)(C_6H_4-CH_3)]; S_4OPH_2, [C(5)(C_6H_4-CH_3)]-[C_4H_2N(42)]-[C(10)(C_6H_4-CH_3)] (Figure 2 and 5, Table 1). The ^{1}H chemical shifts of thiophene (12-H, 13-H) and pyrrole (7-H, 8-H), (17-H, 18-H) hydrogens of S_4OP are in the range of other nonaromatic conjugated systems which contain thiophene and pyrrole moieties.[10] The chemical shift of these fragments can be considered as reference points for other fragments of S_4OP and S_4OPH_2. The marked upfield shifts are determined for the [C(5)(C_6H_4-CH_3)]-[C_4H_2N(42)]-[C(10)(C_6H_4-CH_3)] fragment in the case of S_4OPH_2 but downfield shifts for [C(40)(C_6H_4-CH_3)]-[C_4H_2S(41)]-[C(5)(C_6H_4-CH_3)] of S_4OP or even more prominent for its dication, $S_4OPH_2^{2+}$. The position of 2-H and 3-H resonances is strongly solvent dependent as exemplified by the ^{1}H NMR spectrum of S_4OP in [D_8]toluene. The 2-H and 3-H resonances are located at $\delta = 10.97$ and $\delta = 7.82$ ([D_8]toluene, 294 K), that is considerably downfield with respect to the corresponding values measured in [D_2]dichloromethane (Table 1). The shift differences between the 2-H, 3-H and 12-H, 13-H thiophene resonances of S_4OP or 7-H, 8-H and 17-H, 18-H pyrrole resonances of S_4OPH_2 reflect the substantial anisotropy of the shielding-deshielding macrocyclic effect. Significantly, the sign of anisotropy is reversed going from S_4OPH_2 to S_4OP.

Originally it was noticed that the 3-H resonance of S_4OP is in an unusually downfield position even in comparison to the adjacent 2-H resonance, which is located on the same thiophene ring. However, both are considerably downfield shifted with reference to the shifts of 12-H and 13-H resonances. The upfield component, present for the 2-H resonance, which originates from the local 40-*p*-tolyl ring current effect, is missing in the shift of 3-H because of the unusual position of the 5-*p*-tolyl ring. This structural difference may account in part for the spectroscopic features of the 2-H – 3-H couple.

Dihydrotetrathiaoctaphyrin contains 38-π electrons in its conjugation pathway that corresponds to the formal $[4n+2]$ Hückel type π electron formulation, in which the overall macrocyclic aromaticity is shown in ^{1}H NMR spectra by notable diatropic ring current effect. Two-electron oxidation of dihydrotetrathiaoctaphyrin yields tetrathiaoctaphyrin which corresponds to the formal $4n$ type π electron formulation which allows the overall macrocyclic antiaromaticity to be revealed in the ^{1}H NMR spectroscopy by paratropic shifts. These considerations imply an assumption of almost planar structures in relation to these that are presented in Scheme 2 and Scheme 3. However, we have already demonstrated that this is not the case. Our results provide evidence that, in the case of 38-π electron and 36-π electron figure-eight tetrathiaoctaphyrins, the correlation between number of π electrons and the nature of ring current effect is, at least qualitatively, preserved although the detected effect is considerably smaller with respect to regular porphyrin and extended porphyrin as well to their heteroanalogues.[9, 17] In their electronic structure, a S_4OPH_2 – S_4OP couple is analogous to the [18]tetraoxaporphyrin dication (O_4P^{2+}) – [20]tetraoxaisophlorin (O_4P) couple, in which two-electron reduction results in a replacement of the diatropic effect by the paratropic one.[36] One has to be aware of the different figure-eight related geometry of the effect as compared to prototypical planar conjugated porphyrin or extended porphyrins. In fact, it has been suggested that lack of aromaticity for $[4n+2]$ [34]octaphyrin(1.1.1.0.1.1.1.0) may result from macrocyclic nonplanarity or other factors such as the ring size or self canceling magnetic moments within each "half" of the molecule.[35] Nevertheless, it has also been demonstrated the hexaanion of figure-eight [28]paracyclophaneoctaene is a 54-π electron diatropic system.[32] Thus, the assumption is that the upper [S(41)N(42)S(43)N(44)] or bottom [S(45)N(46)S(47)-N(48)] moieties of the figure-eight ribbon of dihydrotetrathiaoctaphyrin is the cause of the diatropic effect that creates the resultant shielding zones above and below the {S(41)N(42)S(43)} or {S(45)N(46)S(47)} reference planes. Therefore, the resonances of the [C(5)(C_6H_4-CH_3)]-[C_4H_2N(42)]-{[C(25)(C_6H_4-CH_3)]-[C_4H_2N(46)]} fragment located above the [S(45)N(46)S(47)] {[S(41)N(42)S(43)]} plane of reference should demonstrate the considerable upfield relocation. The effect of the opposite sign is expected at the ribbon-crossing thiophene in S_4OP due to the macrocyclic paratropicity.[37]

Rearrangement processes—rotation of *meso*-*p*-tolyl groups: The temperature dependence of the one-dimensional ^{1}H NMR spectrum of S_4OP is shown in Figure 2.

The two *ortho* and *meta* protons on each *meso* phenyl ring are unequivalent due to the helical structure of S_4OP. Thus each *ortho* or *meta* *p*-tolyl pair should present two separate resonances in the ^{1}H NMR spectra if rotation about the *meso*-carbon–*p*-tolyl bond is restricted. The 5-*p*-tolyl group is located in a rather crowded region of the figure-eight compound (Figure 3). This ring is flanked by pyrrole in a regular orientation and by the thiophene ring, which is inverted with respect to the regular porphyrinic arrangement. The steric hindrance of the thiophene S(41) atom and one β-CH fragment is smaller than that expected for the two β-CH fragments in all other *p*-tolyl groups. This factor may lower the rotation barrier in comparison to other *meso* positions, which results in the selective broadening of 5-*p*-tolyl resonances seen at the 248 – 213 K range (Trace B of Figure 2). Once temperature has been increased above 268 K, broadening of *ortho* and *meta* resonances, as well as those from all

0947-6539/01/0723-5106 $ 17.50+.50/0 *Chem. Eur. J.* **2001**, *7*, No. 23

pyrrole, and thiophenes, is observed to produce the deceptively simplified spectrum at 293 K (Figure 2, Trace C). This renders the specific analysis of *meso p*-tolyl rotation impractical.

Similar spectral changes related to the *meso p*-tolyl rotation have been detected in variable-temperature ^{1}H NMR studies carried out for S_4OPH_2. The dynamic broadening of 5-*p*-tolyl and 20-*p*-tolyl resonance is detected at 293 K in [D]chloroform but rotation is restricted for two other *meso p*-tolyl groups located further away from the ribbon crossing pyrrole rings. The ^{1}H NMR spectra of $SOPH_2$ in [D_8]toluene show that edition of the pyrrole and thiophene resonances is observed as all *p*-tolyl resonances demonstrate severe broadening in constrast to the sharp pyrrole and thiophene resonances.

Rearrangement processes—transformation of figure-eight geometry of S_4OP: The methyl resonances, which are located in the $\delta = 2.2-2.6$ region, present well-defined dynamic behavior by completing a fast exchange step. The four methyl resonances are observed in the 193–273 K temperature range ([D_2]dichloromethane). As the temperature is gradually raised, the 40(20)-Me and 5(25)-Me resonances broaden, coalesce into one broad resonance at $\delta = 2.5$ and finally give one sharp single peak. This behaviour is characteristic of a fast exchange between the 5-Me and 20-Me structural positions (Scheme 4). Simultaneously the similar changes are detected for a 15-Me and 10-Me pair. It is notable that the methyl groups are located on the rotation axis of the *p*-tolyl rings and that the rotational dynamic process is not reflected in the spectroscopic pattern. The rearrangement process evidently excludes, at least in the investigated temperature limits, any exchange between the methyl groups, which belong to two different couples, that is between 5,20-Me and 10,15-Me sets.

All other resonances demonstrate easily recognizable features in one-dimensional ^{1}H NMR spectra that indicate a slow rate exchange process that is severe broadening of all pyrrole and thiophene resonances. We note that a fast exchange rate, which yields well-resolved dynamically averaged spectrum, is not detected for these resonances at the accessible high temperature limits of chlorinated solvents ([D]chloroform, [D_2]dichloromethane) or [D_8]toluene. The chemical shift difference determined for exchangeable methyl pairs ($\delta = 2.52$ for 5-Me and 20-Me; $\delta = 2.39$ for 10-Me and 15-Me) are in the range in which all stages of the exchange process could be seen in the course of experiment. The shift differences for the other dynamic pairs are markedly larger. Consequently only dynamically broadened spectrum could be observed.

The lineshape analysis of the 5,20 pair was carried out using the iterative computer program which yields appropriate rate constants. An approach which assumes an exchange between two equally populated scalar uncoupled pairs was applied.[38] Activation parameters are obtained from the least-squares fits of the rate constants to the Arrhenius and Eyring equations. They are equal: $E_a = 57.9 \pm 1.5$ kJ mol^{-1} $\Delta H^{\neq} = 55.3 \pm 1.5$ kJ mol^{-1}, $\Delta S^{\neq} = -28.0 \pm 5.1$ J K^{-1} mol^{-1}. Analogous analysis, which was carried out on the second dynamic 15,20 methyl pair, gives similar values. The exchange process is solvent dependent. Hence, activation parameters in [D_8]toluene are equal $E_a = 91.9 \pm 2.7$ kJ mol^{-1}) $\Delta H^{\neq} = 89.2 \pm 2.7$ kJ mol^{-1} $\Delta S^{\neq} = 72.6 \pm 8.4$ J K^{-1} mol^{-1}.

The $\Delta G^{\neq}_{298} = 63.6 \pm 3.0$ kJ mol^{-1} ([D]chloroform) or $\Delta G^{\neq}_{298} = 67.6 \pm 5.2$kJ mol^{-1} ([$D_8$]toluene) values are considerably smaller when calculated from NMR data ($\Delta G^{\neq} \gg 85$ kJ mol^{-1}) or when measured directly ($\Delta G^{\neq}_{298} = 96.5$ kJ mol^{-1} for [36]octaphyrin(2.1.0.1.2.1.0.1).[6, 7] These data have initiated a discussion on the rearrangement mechanism of a tetrathiaoctaphyrin in light of previously documented structural flexibility of figure-eight molecules.[6, 8, 7, 34b–d]

In spite of the obvious structural similarities the figure-eight transformation that is observed in S_4OP is not observed in S_4OPH_2 in [D_2]dichloromethane.

Rearrangement mechanisms: To account for the dynamic behavior of S_4OP we have considered two mechanisms: 1) fast dynamic equilibrium, which includes helix inversion, between two enatiomeric forms of the double helical figure-eight S_4OP; 2) a figure-eight conveyor-belt-like movement of the whole ring without a racemization step.

The first mechanism is based on fast exchange between two limiting enantiomeric conformations (Scheme 6). These conformations can interconvert via left- or right-handed twists along the long axis as shown in Scheme 6. The process includes a presumed open pseudo-circular intermediate as the crucial step of a rearrangement route. Such a seemingly straightforward racemization requires concerted rotations of

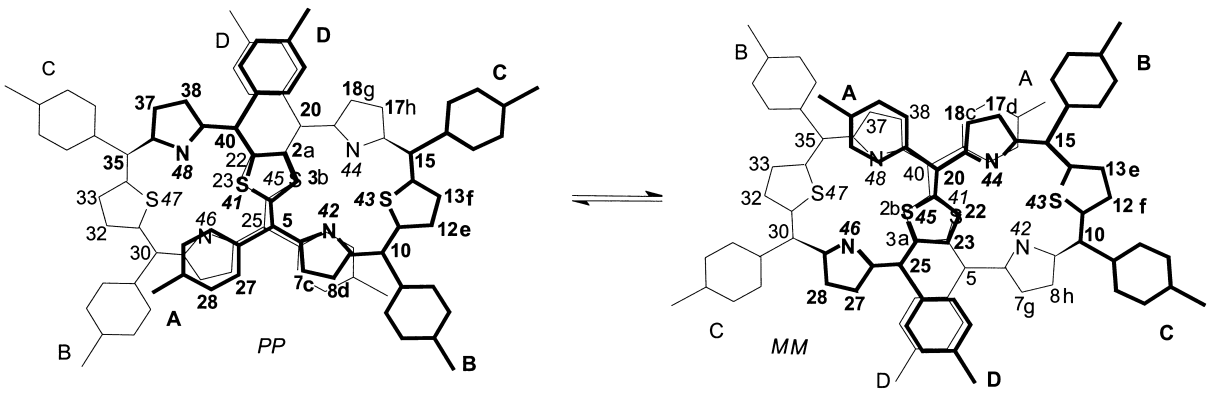

Scheme 6. An exchange between two limiting enantiomeric conformations of S_4OP.

the molecule using a route that minimizes the steric hindrance of the *p*-tolyl groups.

For the convenience of further analysis the *p*-tolyl, β-H thiophene and β-H pyrrole groups are systematically labeled (a – h), labels which refer to the characteristic chemical shifts, detected for the *PP* frozen configuration (Scheme 6 and Figure 3). Accordingly the following series of two-site dynamic pairs are anticipated from Scheme 6. Formally, the exchange takes place between two limiting positions with shifts that were determined for the frozen configuration of S_4OP-*PP* as follows: A – D (5-, 20-, 25-, 40-*p*-tol), B – C (10-, 15-, 30-, 35-*p*-tol), a – b (2-H, 3-H, 22-H, 23-H), c – g (7-H, 18-H, 27-H, 38-H), d – h (8-H, 17-H, 28-H, 37-H), e – f (12-H, 13-H, 32-H, 33-H). In the fast exchange limit two A_2 thiophene patterns and one pyrrole AB pattern are expected to be observed as evidence for a time averaged spectroscopic photograph of two limiting C_2 symmetry enantiomers which would lead to the spectrum that corresponds to the effective D_2 symmetry of S_4OP. The hypothetical racemization would preserve the antiperiplanar positions of the C(39)–C(40) and C(5)–C(6) bonds (the improper torsion angle approaches 180°), that is at positions where the helix makes an opposite turn as compared to the regular porphyrin (the relevant C(39)–C(40) and C(5)–C(6) dihedral angles of porphyrin approaches 0°). The racemization would also require an exchange between two equivalent modes of the thiophene – thiophene spacer pyrrole overlap which would result from a fast flipping motion of the two thiophenes spacer groups as shown in Scheme 6. At these projections either C(4)-C(5)-C(25)-C(24) (S_4OP-*PP*) or C(1)-C(40)-C(20)-C(21) (S_4OP-*MM*) improper torsional angles would come close to 0°. Although the fast racemization process could adequately describe the spectroscopic pattern and exchange phenomenon of S_4OP we have noticed that the measured exchange rate is very fast in comparison to turcasarin or octaphyrins.[6, 8, 36] The exchange rate for S_4OP at 297 K equals 42 s^{-1} which contrasts with the value of $k = 7.5 \times 10^{-5}$ obtained at 299 K for [36]octaphyrin(2.1.0.1.2.1.0.1) racemization.[6] Intuitively, one expects that bulky *meso p*-tolyl substituents of S_4OP would slow the racemization process.

An alternative pathway with identical spectroscopic consequences to those described above is considered (Scheme 7). This novel mechanism assumes the preservation of figure-eight chirality but implies a sequence of steps which involve a 180° inversion of the "ribbon crossing" S(41) thiophene ring followed by the analogous flip of S(45) ring. Such a rearrangement should be followed by the figure-eight conveyor-belt-like movement of the whole S_4OP ring in order to reconstruct geometry around the S(41) and S(45)thiophene spacers and consequently the whole tetrathiaoctaphyrin molecule. Accordingly, the molecule shuttles between two energetically and structurally identical forms as shown in Scheme 7. This results in two-site exchange dynamic process in the following pairs: A – D (5-, 20-, 25-, 40-*p*-tolyl), B – C (10-, 15-, 30-, 35-*p*-tolyl), a – b (2-H, 3-H, 22-H, 23-H), c – g (7-H, 18-H, 27-H, 38-H), d – h (8-H, 17-H, 28-H, 37-H), e – f (12-H, 13-H, 32-H, 33-H).

The similar conveyor-type process can be constructed for figure-eight octaphyrins[6, 39] and for the very first giant expanded porphyrins – turcasarin.[8, 40]

S_4OP – S_4OPH_2 redox-dependent transformation of the figure-eight geometry: Dihydrogenation of S_4OP to S_4OPH_2 or oxidation of S_4OPH_2 to S_4OP is linked to a profound structural change. The $S_4OP \rightarrow (\leftarrow)$ S_4OPH_2 process can be considered as a sequence of two-electron reduction (two-electron oxidation) and protonation (deprotonation) steps. Thus a $S_4OP - S_4OPH_2$ couple can be treated as a redox-switching molecule, which, while preserving the overall figure-eight geometry, "chooses" pyrrole or thiophene rings as spacers as a function of the macrocyclic oxidation state.

The $S_4OP - S_4OPH_2$ rearrangement mechanism, which is triggered by a redox change and produces the unstable S_4OPH_2 configuration, S_4OPH_2*, preserves the figure-eight chirality but requires a sequence of steps which involve a $\approx$180° rotation of the C(25)-$C_6H_4CH_3$ fragment followed by $\approx$ 180° flip of C(5)-$C_6H_4CH_3$. Consequently, the S(41) and S(45) thiophene "zigzags" are replaced by the N(42) and N(46) pyrrole "zigzags" respectively. Such a rearrangement must by accompanied by two inversions of the N(42) and N(46) pyrroles and a figure-eight conveyor-belt-like movement of the entire S_4OPH_2 ring to reconstruct the geometry around the new N(42) and N(46) pyrrole spacers and consequently the whole dihydrotetrathiaoctaphyrin molecule as shown in Scheme 8. One of the several feasible asymmetric intermediate configurations is also presented in Scheme 8.

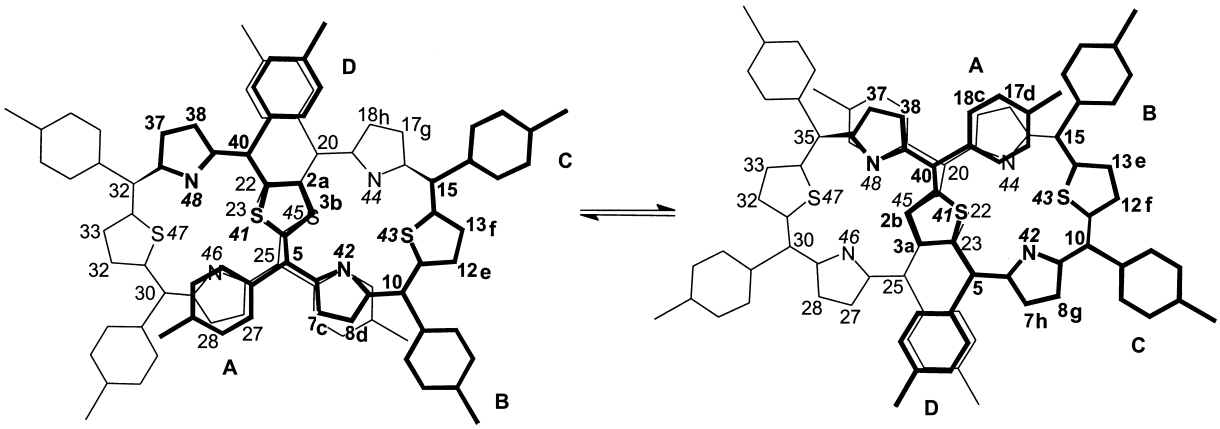

Scheme 7. An alternative rearrangement pathway of figure-eight tetrathiaoctaphyrin.

  0947-6539/01/0723-5108 $ 17.50+.50/0 *Chem. Eur. J.* **2001**, *7*, No. 23

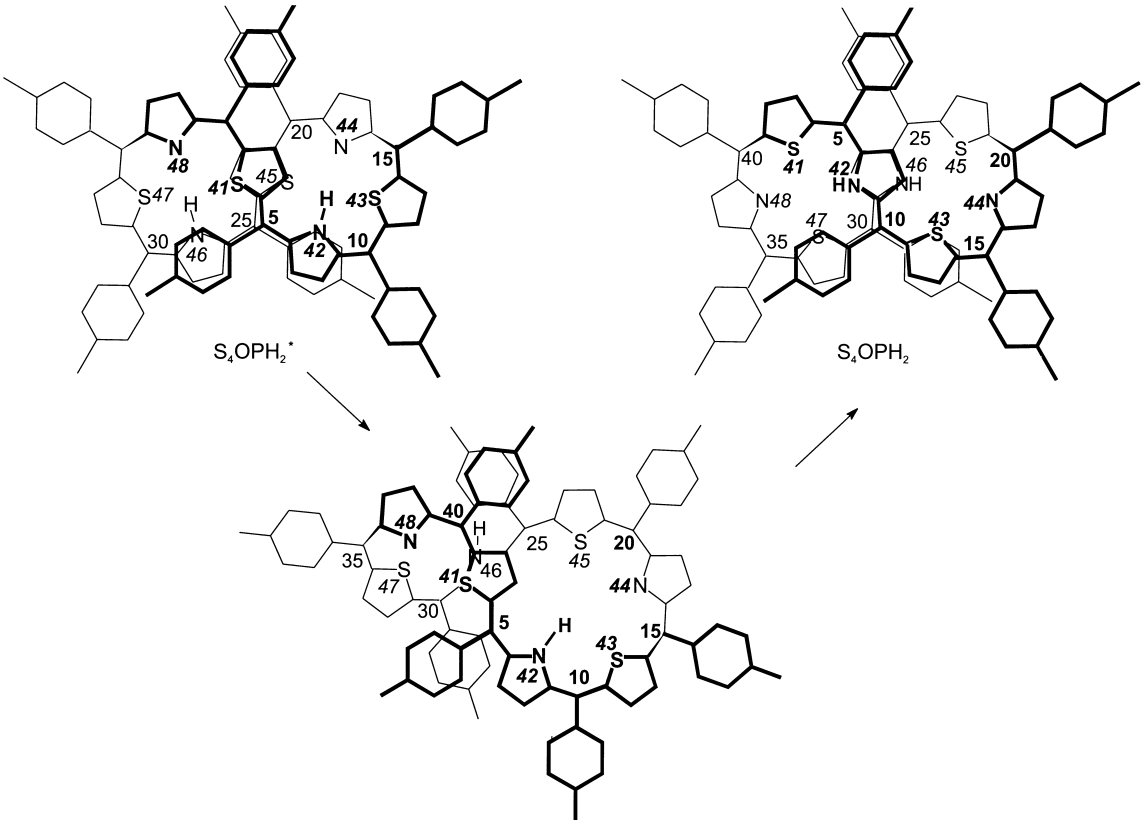

Scheme 8. Rearrangement that occurs, which is accompanied by two inversions of the N(42) and N(46) pyrroles and a figure-eight conveyor-belt-like movement of the entire S_4OPH_2 ring, to reconstruct the geometry of dihydrotetrathiaoctaphyrin. One of the several feasible asymmetric intermediate configurations is also presented.

Formation of figure-eight tetrathiaoctaphyrin: The formation of figure-eight giant heteroporphyrins S_4OPH_2 and S_4OP can be accounted for by a mechanism of Rothemund-type condensation. However, instead of the typically preferred porphyrin or heteroporphyrin structures, doubly large cyclic molecules are synthesized.[15, 16, 25]

Analogous to other modifications of the Rothemund synthesis, we suggest that a mixture of dithiaanalogues of tetrapyrromethane form at equilibrium. These intermediate compounds are expected to preserve the preferred helical conformation of tetrapyrromethane.[41, 42] Two pre-constructed enantiomeric building fragments are suggested for the construction of large macrocycles by the synthesis of octaphyrin. They are differentiated by helicity as shown in Figure 7. The helical geometry of the open *P* or *M* precursor provides the orientation required for the formation of two covalent bonds to form figure-eight tetrathiaoctaphyrinogen, which can be subsequently oxidized to dihydrotetrathiaoctaphyrin and tetrathiaoctaphyrin. The *P*–*P* or *M*–*M* combinations are presumably preferred for steric reasons in the formation the enantiomeric figure-eight molecule rather than the *P*–*M* combination, which would produce a optically inactive "squeezed-eight" *meso*-structure.

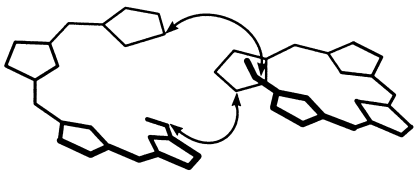

Figure 7. The orientation of the two *P* enantiomers of the dithiaanalogue of tetrapyrromethane represents a suggested step in the synthesis of tetrathiaoctaphyrinogen, in which the formation of tetrathiaoctaphyrinogen is preferred rather than intramolecular dithiaporphyrinogen ring closure. The helical structure of the *P* enantiomer has been obtained from molecular mechanics calculations.

Conclusion

The acid-catalyzed condensation of pyrrole and 2,5-bis(phenylhydroxymethyl)thiophene yields, apart from the well-known dithiaporphyrin, two novel members of the giant porphyrin family: tetrathiaoctaphyrin and dihydrotetrathiaoctaphyrin. The spectroscopic evidence indicates that both compounds possess helical figure-eight geometry. The protonation mechanism reflects the unusual structure of the molecule. Two dithiaporphyrin-like pockets behave as independent proton acceptors. The stepwise process yields symmetric or asymmetric cationic species depending on number of added protons.

Dihydrotetrathiaoctaphyrin contains 38 π electrons in its conjugation pathways which corresponds to the formal $[4n+2]$ Hückel type π-electron formulation. This suggests that the overall macrocyclic aromaticity is demonstrated in its ^{1}H NMR spectra by the residual diatropic ring current effect. Two-electron oxidation of dihydrotetrathiaoctaphyrin yielded tetrathiaoctaphyrin which corresponds to the formal $4n$ type π-electron formulation and suggests that the overall macro-

cyclic antiaromaticity is revealed by small paratropic shifts. Variable-temperature ^{1}H NMR experiments provided evidence for the rearrangement processes of S_4OP. To account for the dynamic properties of S_4OP, a novel mechanism was proposed which involves the figure-eight conveyor-belt-like movement of the whole ring without a racemization step. Therefore, the molecule shuttles between two degenerate forms. In the next stage of development, a symmetry-lowering substitution may lead, in principle, to a molecular shuttle which can act as a switch betweeen two non degenerate quasi-stabile molecular states.[43]

In fact, the $S_4OP-S_4OPH_2$ couple may be considered as a redox switch which, while preserving the overall figure-eight geometry, reversibly selects either pyrrole or thiophene rings as spacers as a function of the macrocyclic oxidation state.

Experimental Section

Preparation of precursors: 2,5-Bis(*p*-tolylhydroxymethyl)thiophene was synthesized according to known procedures.[15e]

Synthesis of 5,10,15,20,25,30,35,40-octa-(*p*-tolyl)-41,43,45,47-tetrathia[36]octaphyrin(1.1.1.1.1.1.1.1) (S_4OP): 2,5-Bis(*p*-tolylhydroxymethyl)-thiophene (600 mg, 1.85 mmol) and pyrrole (0.128 mL, 1.85 mmol) were added to freshly distilled dichloromethane (250 mL). N_2 gas was bubbled through the solution for 20 min to remove oxygen before methanesulfonic acid (0.095 mL) was added. The solution was stirred for 1 h in the absence of light, *p*-chloranil (1.35 g, 5.5 mmol) was added, and the solution was heated under reflux (1 h). The solvent was evaporated under reduced pressure. The residue was dissolved in dichloromethane and chromatographed on a basic alumina column. The first red fraction, which contained S_2TTP was removed, and the second fraction, which contained S_4OP, was eluted with dichloromethane. The third fraction, which contained S_4OPH_2 and some impurities, was eluted with a mixture of chloroform and methanol (90/10 v/v). The second fraction was subjected to further chromatography on basic alumina. Fractions eluted with dichloromethane were monitored by UV/Vis spectroscopy and S_4OP eluted as a marine green solution with a yield of 2%. UV/Vis ([D$_2$]dichloromethane): (λ_{max}[nm] (log ε)): 427 (4.59), 631 (4.74); ^{1}H NMR (500 MHz, 213 K, [D$_2$]dichloromethane): $\delta = 10.05$ (d, ^3J(A,B) = 4.4 Hz; 3-H, th.), 8.08 (d, $^3J = 8$ Hz; 5-*o*-Tol.), 7.63 (d, $^3J = 7.8$ Hz; 10-*o*-Tol.), 7.44 (d, $^3J = 7.8$ Hz; 5-*m*-Tol.), 7.40 (d, $^3J = 7.6$ Hz; 20-*m*-Tol.), 7.35 (d, $^3J = 7.8$ Hz; 10-*m*-Tol.), 7.32 (d, $^3J_{(A,B)} = 4.6$ Hz; 2-H, th.), 7.30 (d, $^3J = 7.9$ Hz; 15-*o*′-Tol.), 7.22 (d; 15-*m*′-Tol.), 7.20 (d; 20-*m*′-Tol.), 7.17 (d; 10-*m*′-Tol.), 7.15 (d, $^3J = 7.6$ Hz; 5-*m*′-Tol.), 7.12 (d, $^3J = 7.8$ Hz; 15-*m*-Tol.), 7.06 (d, $^3J = 7.6$ Hz; 20-*o*-Tol.), 7.02 (d, $^3J = 7.6$ Hz; 5-*o*′-Tol.), 6.98 (d; 20-*o*′-Tol.), 6.96 (d; 15-*o*-Tol.), 6.90 (d, $^3J = 7.8$ Hz; 10-*o*′-Tol.), 6.73 (d, ^3J(A,B) = 5.9 Hz; 12-H, th.), 6.62 (d, ^3J(A,B) = 5.7 Hz; 13-H, th.), 6.60 (d, ^3J(A,B) = 4.3 Hz; 7-H, pyrr.), 6.49 (d, ^3J(A,B) = 4.6 Hz; 18-H, pyrr.), 6.47 (d, ^3J(A,B) = 4.3 Hz; 8-H, pyrr.), 6.17 (d, ^3J(A,B) = 4.4 Hz; 17-H, pyrr.), 2.52 (s; CH_3; 20-*p*-Tol.), 2.44 (s; CH_3; 5-*p*-Tol.), 2.38 (s; CH_3; 10-*p*-Tol.), 2.33 (s; CH_3; 15-*p*-Tol.).

$S_4OPH_2^{2+}$: ^{1}H NMR (500 MHz, 196 K, [D$_2$]dichloromethane): $\delta = 10.17$ (s; NH), 9.39 (d, ^3J(A,B) = 4.4 Hz; 3-H, th.), 8.88 (d, $^3J = 7.0$ Hz; 5-*o*-Tol.), 8.50 (d, $^3J = 7.5$ Hz; 5-*m*-Tol.), 8.31 (d, ^3J(A,B) = 4.2 Hz; 2-H, th.), 8.16 (d, $^3J = 6.6$ Hz; 20-*o*-Tol.), 8.10 (d, $^3J = 6.8$ Hz; 10-*o*-Tol.), 7.56 (d, $^3J = 6.6$ Hz; 10-*m*-Tol.), 7.47 (d, $^3J = 6.6$ Hz; 20-*m*-Tol.), 7.42 (5-*m*′-Tol.), 7.32–7.03 (Tol.), 7.41 (8-H pyrr.), 7.29 (7-H, pyrr.), 6.99 (d, ^3J(A,B) = 4.6 Hz; 18-H, pyrr.), 6.89 (d, ^3J(A,B) = 4.4 Hz; 17-H, pyrr.), 6.83 (d, $^3J = 6.8$ Hz; Tol.), 6.52 (d, $^3J = 6.8$ Hz; 10-*o*′-Tol.), 6.42 (d, ^3J(A,B) = 4.2 Hz; 13-H, th.), 6.17 (d, ^3J(A,B) = 4.2 Hz; 12-H, th.), 2.74 (s; CH_3, 20-*p*-Tol.), 2.69 (s; CH_3, 5-*p*-Tol.), 2.44 (s; CH_3, 10-*p*-Tol.), 2.34 (s; CH_3, 15-*p*-Tol.); HRMS (ESI): *m*/*z* calcd for $C_{96}H_{73}N_4S_4$: 1409.4713; found: 1409.4573 [*M*H]$^+$.

S_4OPH_2: 5,10,15,20,25,30,35,40-Octa-(*p*-tolyl)-41,43,45,47-tetrathia[38]dihydrooctaphyrin(1.1.1.1.1.1.1.1) (S_4OP) (2 mg) was reduced with a suspension of sodium borohydride in THF. The progress of the reaction was monitored by UV spectroscopy until the reduction was complete (≈20 min). The reaction was quenched with water and the product extracted with dichloromethane. The extract was evaporated to dryness and the residue subjected to column chromatography on basic alumina. The green fraction, which contained S_4OPH_2, eluted with chloroform/methanol (90/10 v/v). The reaction produced S_4OPH_2 in almost quantitative yield. UV/Vis ([D$_2$]dichloromethane): λ_{max}[nm] (log ε): 346 (4.58), 435 (4.95), 522 (4.07), 567 (4.14), 739 (5.24), 927 (4.08); ^{1}H NMR (500 MHz, 253 K, [D$_2$]dichloromethane): $\delta = 8.25$ (d, $^3J = 7.9$ Hz; 15-*o*-Tol.), 7.93 (d, $^3J = 7.7$ Hz; 20-*o*-Tol.), 7.54 (d, ^3J(A,B) = 5.3 Hz; 13-H, th.), 7.52 (d, $^3J = 7.9$ Hz; 5-*o*′-Tol.), 7.51 (d, ^3J(A,B) = 5.0 Hz; 23-H, th.), 7.48 (d, $^3J = 7.2$ Hz; 15-*m*-Tol.), 7.43 (d, $^3J = 7.9$ Hz; 20-*m*-Tol.), 7.30 (d, $^3J = 7.9$ Hz; 20-*m*′-Tol.), 7.28 (d, $^3J = 7.2$ Hz; 20-*o*′-Tol.), 7.24 (d, $^3J = 7.7$ Hz; 15-*m*′-Tol.), 7.04 (d$^3J = 7.6$ Hz; 5-*m*′-Tol.), 7.00 (17, 18-H, pyrr.), 6.97 (d, ^3J(A,B) = 4.8 Hz; 22-H, th.), 6.94 (d, $^3J = 7.7$ Hz; 15-*o*′-Tol.), 6.81 (d, ^3J(A,B) = 4.3 Hz; 12-H, th.), 6.62 (d, $^3J = 7.6$ Hz; 10-*o*-Tol.), 6.47 (d, $^3J = 7.6$ Hz; 5-*m*-Tol.), 6.43 (d; 10-*m*-Tol.), 5.46 (d; 5-*o*-Tol.), 5.36 (s; NH), 5.27 (d, $^3J = 7.5$ Hz; 10-*m*′-Tol.), 4.46 (d, $^3J = 7.8$ Hz; 10-*o*-Tol.), 4.37 (d, ^3J(A,B) = 5.3 Hz; 8-H pyrr.), 4.18 (d, ^3J(A,B) = 5.1 Hz; 7-H, pyrr.), 2.48 (s; CH_3, 20-*p*-Tol.), 2.47 (s; CH_3, 15-*p*-Tol.), 2.30 (s; CH_3, 5-*p*-Tol.), 1.36 (s; CH_3, 10-*p*-Tol.).

$S_4OPH_3^+$: ^{1}H NMR (500 MHz, 218 K, [D$_2$]dichloromethane): $\delta = 8.36$, 8.34 (d, $^3J = 7.9$ Hz; 15,35-*o*-Tol.), 8.08, 8.00 (d, $^3J = 7.7$ Hz; 20, 40-*o*-Tol.), 7.71, 7.68, 7.64 (d, ^3J(A,B) = 5.3 Hz; 13,23, 33,43 H, th.), 7.61–7.27 (Tol.), 7.05, 7.01 (d; 5,25-*m*′-Tol.), 7.27–6.93 (17,18,37,38-H, pyrr; 12,22,32,42-H, th.), 6.91, 6.84 (d; 15,35-*o*′-Tol.), 6.74, 6.69 (d; 10,30-*o*-Tol.), 6.43, 6.40 (d; 5,25-*m*-Tol.), 6.48, 6.40 (d; 10,30-*m*-Tol.), 5.93, 5,51 (s; NH), 5.39, 5.25 (d; 5-*o*-Tol), 5.36 (s; NH), 5.07, 5.05 (d; 10-*m*′-Tol.), 4.07, 4.05 (d, $^3J = 7.2$ Hz; 10-*o*′-Tol.), 4.48, 3.78 (d, ^3J(A,B) = 4.8 Hz; 8-H pyrr.),4.36 (s; NH), 4.29. 3.63 (d, ^3J(A,B) = 4.6 Hz; 7-H, pyrr.), 2.50 2.48 (s; CH_3, 20, 40-*p*-Tol.), 2.48, 2.47 (s; CH_3, 15, 35-*p*-Tol.), 2.30, 2.28 (s; CH_3, 5, 25-*p*-Tol), 1.26, 1.09 (s; CH_3, 10, 30-*p*-Tol.).

$S_4OPH_4^{2+}$: ^{1}H NMR (500 MHz, 213 K, [D$_2$]dichloromethane): $\delta = 8.51$ (d, $^3J = 7.8$ Hz; 15-*o*-Tol.), 8.17 (d, $^3J = 7.6$ Hz; 20-*o*-Tol.), 8.13, 7.91 (d, ^3J(A,B) = 5.0 Hz; 13,23-H, th.), 7.64 (d, ^3J 8.0 Hz; 15-*m*-Tol.), 7.56 (d; 20-*m*-Tol. 5-*o*′-Tol.), 7.50, 7.45 (20-*m*′-Tol., 20-*o*′-Tol.), 7.33, 7.12 (d, ^3J(A,B) = 4.4 Hz; 17, 18-H, pyrr.), 7.32 (,12, 22-H, th.), 7.31 (15-*m*′-Tol.), 7.07 (d, $^3J = 8.0$ Hz; 5-*m*′-Tol.), 6.84 (d, $^3J = 7.6$ Hz; 15-*o*′-Tol.), 6.63 (d, $^3J = 7.3$ Hz; 10-*o*-Tol.), 6.45 (d, $^3J = 7.8$ Hz; 5-*m*-Tol.), 6.31 (d, $^3J = 7.8$ Hz 10-*m*-Tol.), 5.63 (s; NH), 5.28 (d; 5-*o*-Tol.), 5.10 (d, $^3J = 7.8$ Hz; 10-*m*′-Tol.), 4.93(s; NH), 4.02 (10-*o*-Tol., 7, 8-H pyrr.), 2.53 (s; CH_3, 20-*p*-Tol.), 2.51 (s; CH_3, 15-*p*-Tol.), 2.32 (s; CH_3, 5-*p*-Tol.), 0.95 (s; CH_3, 10-*p*-Tol.).

$S_4OPH_4^{2+}$: ^{1}H NMR (500 MHz, 273 K, [D$_2$]dichloromethane): $\delta = 4.07$, 4.08 (7,8-H, pyrr.), 3.98 (10-*o*-Tol.); HRMS (ESI): *m*/*z* calcd. for $C_{96}H_{75}N_4S_4$ = 1411.4869; found 1411.4903 $[M+H]^+$.

Preparation of samples: [D$_2$]Dichloromethane and [D]chloroform for the NMR samples were passed through basic alumina column before use. The solution of the trifluroacetic acid (TFA) in [D$_2$]dichloromethane was added by syringe to the ^{1}H NMR tube, containing S_4OP or S_4OPH_2. The progress of the reaction was followed by ^{1}H NMR spectroscopy. Typically the titration was carried out at 213 K. The spectra of samples, which predominantly contained the single cationic species, were measured at several temperatures.

Instrumentation: NMR spectra were recorded on a Bruker Avance 500 spectrometer. Absorption spectra were recorded on a diode array Hewlett Packard 8453 spectrometer.

Mass spectra were recorded on an AD–604 spectrometer using the electron impact and liquid matrix secondary ion mass spectrometry techniques. MCD spectra were recorded on a Jasco J-715 Spectropolarimeter.

Molecular mechanics calculations: Molecular mechanics calculations were carried out with HyperChem software(Autodesk). The standard *MM*+ force field was applied.

Acknowledgements

Financial support from the State Committee for Scientific Research KBN of Poland (Grant 3 T09A 155 15) and the Foundation for Polish Science is kindly acknowledged.

  0947-6539/01/0723-5110 $ 17.50+.50/0 *Chem. Eur. J.* **2001**, *7*, No. 23

[1] a) J. -I. Setsune, Y. Katakami, N. Iizuna, *J. Am. Chem. Soc.* **1999**, *121*, 8957; b) J. -I. Setsune, S. Maeda, *J. Am. Chem. Soc.* **2000**, *122*, 12405.

[2] T. D. Lash, *Angew. Chem.* **2000**, 112, 1833; *Angew. Chem. Int. Ed.* **2000**, *39*, 1763.

[3] a) J. L. Sessler, S. J. Weghorn, T. Morishima, M. Rosingana, V. Lynch, V. Lee, *J. Am. Chem. Soc.* **1992**, *114*, 8306; b) B. Lament, J. Dobkowski, J. L. Sessler, S. J. Weghorn, J. Waluk, *Eur. J. Chem.* **1999**, *5*, 3039.

[4] J. L. Sessler, D. Seidel, V. Lynch, *J. Am. Chem. Soc.* **1999**, *121*, 11257.

[5] M. Bröring, J. Jendrny, L. Zander, H. Schmickler, J. Lex, Y. -D. Wu, M. Nendel, J. Chen, D. A. Plattner, K. N. Houk, E. Vogel, *Angew. Chem.* **1995**, *107*, 2709; *Angew. Chem. Int. Ed.* **1995**, *34*, 2515.

[6] E. Vogel, M. Bröring, J. Fink, D. Rosen, H. Schmickler, J. Lex, K. W. K. Chan, Y. -D. Wu, D. A. Plattner, M. Nendel, K. N. Houk, *Angew. Chem.* **1995**, *107*, 2705; *Angew. Chem. Int. Ed.* **1995**, *34*, 2511.

[7] A. Werner, M. Michels, L. Zander, J. Lex, E. Vogel, *Angew. Chem.* **1999**, *111*, 3866; Angew. *Chem. Int. Ed.* **1999**, *38*, 3650.

[8] J. L. Sessler, S. J. Weghorn, V. Lynch, M. R. Johnson, *Angew. Chem.* **1994**, *106*, 1572; *Angew. Chem. Int. Ed.* **1994**, *33*, 1509.

[9] J. L. Sessler, A. Gebauer, S. J. Weghorn, "Expanded Porphyrins" in *The Porphyrin Handbook*, *Vol. 2* (Eds.: K. M. Kadish, K. M. Smith, R. Guilard), Academic Press, New York, **2000**, p. 55. See ref. [147] within ref. [9].

[10] M. Kozaki, J. P. Parakka, M. P. Cava, *J. Org. Chem.* **1996**, *61*, 3657.

[11] V. Rao, G. Anand, S. K. Pushpan, A. Srinvasan, S. J. Narayanan, B. Sridevi, T. K. Chandrashekar, R. Roy, B. S. Joshi, *Org. Lett.* **2000**, *2*, 3829.

[12] J. Krömer, I. Rios -Carreras, G. Fuhrmann, C. Musch, M. Wunderlin, T. Debaerdemaeker, E. Mena-Osteriz, P. Bäuerle, *Angew. Chem.* **2000**, *112*, 3623; *Angew. Chem. Int. Ed.* **2000**, *39*, 3481.

[13] a) P. Rothemund, *J. Am. Chem. Soc.* **1936**, *58*, 625; b) P. Rothemund, *J. Am. Chem. Soc.* **1939** *61*, 2912; c) P. Rothemund, A. R. Menotti, *J. Am. Chem. Soc.* **1941**, *63,* 267.

[14] J. Lindsey, "Synthesis of *meso*-Substituted Porphyrins" in *The Porphyrin Handbook*, *Vol. 1* (Eds.: K. M. Kadish, K. M. Smith, R. Guilard), Academic Press, New York, **2000**, p. 45.

[15] a) A. Ulman, J. Manassen, *J. Am. Chem. Soc.* **1975**, *97*, 6540; b) A. Ulman, J. Manassen, F. Frolow, D. Rabinovich, *Tetrahedron Lett.* **1978**, 167; c) A. Ulman, J. Manassen, F. Frolow, D. Rabinovich, *Tetrahedron Lett.* **1978**, 1885; d) A. Ulman, J. Manassen, F. Frolow, D. Rabinovich, *J. Am. Chem. Soc.* **1979**, *101*, 7055; e) A. Ulman, J. Manassen, *J. Chem. Soc. Perkin Trans. 1* **1979**, 1066.

[16] a) P. J. Chmielewski, L. Latos-Grażyński, M. M. Olmstead, A. L. Balch, *Chem. Eur. J.* **1997**, *3*, 268; b) E. Pacholska, L. Latos-Grażyński, Z. Ciunik, *Angew. Chem.* **2001**, issue 23; *Angew. Chem. Int. Ed.* **2001**, issue 23, in press.

[17] L. Latos-Grażyński, "Core Modified Heteroanalogues of Porphyrins and Metalloporphyrins" in *The Porphyrin Handbook*, *Vol. 2* (Eds.: K. M. Kadish, K. M. Smith, R. Guilard), Academic Press, New York, **2000**, p. 361.

[18] a) L. Latos -Grażyński, J. Lisowski, M. M. Olmstead, A. L. Balch, *J. Am. Chem. Soc.* **1987**, *109*, 4428; b) L. Latos -Grażyński, E. Pacholska, P. J. Chmielewski, M. M. Olmstead, A. L. Balch, *Angew. Chem.* **1995**, *107*, 2467; *Angew. Chem. Int. Ed.* **1995**, *34*, 2252; c) L. Latos-Grażyński, E. Pacholska, P. J. Chmielewski, M. M. Olmstead, A. L. Balch, *Inorg. Chem.* **1996**, *35*, 566.

[19] a) A. Srinivasan, B. Sridevi, M. V. R. Reddy, S. J. Narayanan, T. K. Chandrashekar, *Tetrahedron Lett*. **1997**, *38*, 4149; b) B. Sridevi, S. J. Narayanan, A. Srinivasan, M. V. Reddy, T. K. Chandrashekar, *J. Porphyrins Phthalocyanines* **1998**, *2*, 69.

[20] a) P. J. Chmielewski, L. Latos-Grażyński, K. Rachlewicz, T. Glowiak, *Angew. Chem.* **1994**, *106*, 805; *Angew. Chem. Int. Ed.* **1994**, *33*, 779; b) H. Furuta, T. Asano, T. Ogawa, *J. Am. Chem. Soc.* **1994**, *116*, 767.

[21] P. J. Chmielewski, L. Latos-Grażyński, K. Rachlewicz, *Eur. J. Chem.* **1995**, *1*, 68.

[22] a) E. Rose, A. Kossanyi, M. Quelquejeu, M. Soleilhavoup, F. Duwavran, N. Bernard, A. Lecas, *J. Am. Chem. Soc.* **1996**, *118*, 1567; b) L. Latos-Grażyński, P. J. Chmielewski, *New J. Chem.* **1997**, *21*, 691; c) Z. Gross, N. Galili, I. Saltzman, *Angew. Chem.* **1999**, *111*, 1530; *Angew. Chem. Int. Ed.* **1999**, *38*, 1427; d) R. Paloesse, L. Jaquinod, D. J. Nurco, S. Mini, F. Sagone, T. Boschi, K. M. Smith, *Chem. Commun.* **1999**, 1307.

[23] M. G. P. M. S. Neves, R. M. Martins, A. C. Tomé, A. J. D. Silvestre, A. M. S. Silva, V. Félix, M. G. B. Drew, J. A. S. Cavaleiro, *Chem. Com.* **1999**, 385.

[24] J. -Y. Shin, Yonezawa, H. Furuta, A. Osuka, *Abstracts of the 1*st *International Conference on Porphyrins and Phtalocyanines*, POST562, Dijon, June **2000**.

[25] K. Rachlewicz, N. Sprutta, P. J. Chmielewski, L. Latos-Grażyński, *J. Chem. Soc. Perkin 2* **1998**, 969.

[26] S. J. Narayanan, B. Sridevi, T. K. Chandrashekar, A. Vij, R. Roy, *J. Am. Chem. Soc.* **1999**, *121*, 9053.

[27] a) W. -S. Cho, H. -J. Kim, B. J. Littler, M. A. Miller, C. -H. Lee, J. -S. Lindsey, *J. Org. Chem.* **1999**, *64*, 7890; b) B. Sridevi, S. J. Narayanan, T. K. Chandrashekar, U. Englich, K. Ruhlandt-Senge, *Chem. Eur. J.* **2000**, *6*, 2554.

[28] N. Sprutta, L. Latos -Grażyński *Org. Lett.* **2001**, *3*, 1933.

[29] J. L. Sessler, A. Gebauer, S. J. Weghorn, "Expanded Porphyrins" in *The Porphyrin Handbook*, *Vol. 2* (Eds.: K. M. Kadish, K. M. Smith, R. Guilard), Academic Press, New York, **2000**, 101.

[30] U. Knof, A. Von Zelewsky, *Angew. Chem.* **1999**, *111*, 312; Angew. *Chem. Int. Ed.* **1999**, *38*, 302.

[31] B. Thulin, O. Wennerström, *Acta Chem. Scand.* **1976**, *B30*, 688.

[32] R. Schenk, K. Müllen, O. Wennerström, *Tetrahedron Lett.* **1990**, *31*, 7367.

[33] a) D. Ranganathan, V. Haridas, R. Nagaraj, I. L. Karle, *J. Org. Chem*. **2000**, *65*, 4415; b) M. Mascal, C. J. Moody, A. I. Morrel, A. M. Z. Slawin, D. Williams, *J. Am. Chem. Soc.* **1993**, *115*, 813; c) F. J. Schmitz, M. B. Ksebati, J. S. Chang, J. L.Wang, M .B. Hossain, D. van der Helm, M. H. Engel, A. Serban, J. A. Silfer, *J. Org. Chem*. **1989**, *54*, 3463; d) T. Ischida, Y. In, F. Shinozaki, M. Doi, D. Yamamoto, Y. Hamada, T. Shiori, M. Kamigauchi, M. Sugiura, *J. Org. Chem*. **1995**, *60*, 3994; e) P. Wipf, P. C. Fritch, S. J. Geib, A. M. Sefler, *J. Am. Chem. Soc.* **1998**, *120*, 4105.

[34] a) N. Belfrekh, C. Dietrich-Buchecker, J. Sauvage, *Inorg. Chem*. **2000**, *39*, 5169; b) P. Comba, A. Kühner, A. Peters *J. Chem. Soc. Dalton Trans.* **1999**, 509; c) D. E. Fenton, R. W. Matthews, M. McPartin, B. P. Murphy, I. J. Scowen, P. A. Tasker, *Chem. Commun.* **1994**, 1391; d) P. Comba, A. Fath, T. W. Hambley, A. Kühner, D. T. Richens, A. Vielfort, *Inorg. Chem*. **1998**, *37*, 4389.

[35] a) E. Vogel *Pure Appl. Chem.* **1993**, *66*, 143; b) E. Vogel *J. Heterocyclic Chem.* **1996**, *33,* 1461; c) N. Pohl, H. Schmickler, J. Lex, E. Vogel, *Angew. Chem.* **1991**, *103,* 1665; *Angew. Chem. Int. Ed.* **1991**, *30*, 1693.

[36] J. L. Sessler, S. J. Weghorn, *Expanded, Contracted and Isomeric Porphyrins* (Pergamon Tetrahedron Organic Chemistry Series) *Vol. 15*, Elsevier, **1997**, p. 378.

[37] The residual diatropic or paratropic effect may operate in any conjugated figure-eight molecules. The characteristic diagnostic chemical shift changes are expected as long as the appropriate spectroscopic probes of dia- or paratropic effect, that is β-H pyrrolic protons, are present in the structure. In fact, unsubstituted pyrrolic fragments are located at the figure-eight crossing center of [40]decaphyrin(0.0.1.0.1.0.0.1.0.1) (turcasarin), that is just above the pentaphyrin-like cavity.[8] The corresponding set of the four, symmetry unequivalent, β-H resonances of turcasarin ($\delta = 7.00, 7.65, 8.68, 9.73$) is quite distinct.[8] As a position at about 6.5 ppm may be predicted for a nonaromatic conjugated system, the spread of the pyrrole resonances and the remarkable downfield position at $\delta = 9.73$ of one resonance can be accounted for solely by the paratropic effect in this giant porphyrin molecule. This conclusion is consistent with the $4n$ π-electron formulation for turcasarin.[8]

[38] a) M. L. Martin, J.-J. Delpuech, G. J. Martin, *Practical NMR Spectroscopy* Heyden, London, Philadelphia, Rheine, 1980; b) J. Heidberg, J. A. Weil, G. A. Janusonis, J. K. Anderson, *J. Chem. Phys.* **1964**, *41*, 1033.

[39] If one considers the analogous step-wise process in the case of the octaethyl[32]octaphyrin(1.0.1.0.1.0.1.0), [5] which contains four bipyrrolic fragments that are bridged symmetrically by methine bonds, the process would involve the reversible 180° inversion of the pyrrole ring of bipyrrolic and attached methine fragments. In several correlated steps, bipyrrolic units located in the crossing center and at the [32]octaphyrin(1.0.1.0.1.0.1.0) periphery, exchange their position with the conservation of the enantiomeric structure.[5] The helicity of the

figure-eight molecule is protected during this process. Consequently, the methylene protons of the ethyl group remain diasterotopic, which results in their ^{1}H NMR magnetic unequivalence. Thus within the fast exchange limits, one observes a spectrum containing two ABX_3 patterns.[8] This mechanism allows to accept that the racemization process of octaphyrins is slow on the ^{1}H NMR time scale and [32]octaphyrin(1.0.1.0.1.0.1.0),[5] is not exceptional in the class of giant porphyrins in this respect.[36]

[40] The EXSY correlations, which were observed for turcasarin in the NOESY map, can be related to the shuttling of the molecule between two energetically degenerated configuration without inversion of the macrocycle.[8] Two equivalent mutual orientations of the trispyrrolic fragment at the figure-eight crossing center of [40]decaphyrin-(0.0.1.0.1.0.0.1.0.1) are available. The shuttling preserves the unsubstituted pyrrole ring at the central location but two adjacent monoalkylated rings exchange their structural roles.

[41] a) B. Franck, *Angew. Chem.* **1982**, *92*, 327; *Angew. Chem. Int. Ed. Engl.* **1982**, *21*, 343; b) G. Bringmann, B. Franck, *Liebigs. Ann. Chem.* **1982**, 1272; c) G. B. Bringmann, Franck, *Liebigs. Ann. Chem.* **1982**, 1261; d) K. -H. Schumacher, B. Franck, *Angew. Chem.* **1989**, *101*, 1253; *Angew. Chem. Int. Ed.* **1989**, *28*, 1243.

[42] L. F. Tietze, H. Geissler, *Angew. Chem.* **1993**, *105*, 1087; *Angew. Chem. Int. Ed. Engl.* **1993**, *32*, 1038.

[43] a) V. Balzani, M. Gómez -López, J. F. Stoddart, *Acc. Chem. Res.* **1998**, *31*, 405; b) V. Balzani, A. Credi, F. M. Raymo, J. F. Stoddart, *Angew. Chem.* **2000**, *112*, 3484; *Angew. Chem. Int. Ed.* **2000**, *39*, 3349.

Received: February 23, 2001 [F3090]

  0947-6539/01/0723-5112 $ 17.50+.50/0